Superalloys 718, 625, 706 and Derivatives 2005 *Edited by E.A. Loria*
TMS (The Minerals, Metals & Materials Society), 2005

MIXED INCONEL® ALLOY 718 INERTIA WELDS FOR ROTATING APPLICATIONS – MICROSTRUCTURES AND MECHANICAL PROPERTIES

O. Roder[1*], D. Helm[1], S. Neft[1], J. Albrecht[2], G. Luetjering[2]

[1]MTU Aero Engines GmbH, 80995 Munich, Germany
[2]Technical University Hamburg-Harburg, 21073 Hamburg, Germany

Keywords: IN718, Inertia Welding, Microstructure, Mechanical Properties

Abstract

IN718 is the work-horse nickel-iron-chromium alloy for a variety of parts for aero-engine applications such as disks, shafts, blades, vanes, casings and fasteners due to a good combination of relevant mechanical properties, good corrosion resistance, easy fabricability and reasonable cost.
The conditions in aero-engines often require joining rotating parts which are made out of different materials, for example due to temperature limitations of one material. Besides the possibility of bolting the parts together, welding can lead to some advantages and is used in the compressor and high-pressure turbine section of aero-engines. For joining nickel-super-alloys and especially different nickel-alloys inertia welding represents often the only available possibility.
The following work summarizes investigations of inertia welding IN718 with alloys INCOLOY® alloy 909, UDIMET® 720LI, René® 88DT and itself. The influence of various post-weld heat-treatments on the microstructure and some relevant mechanical properties as tensile and low cycle fatigue properties is described. The focus in this work is on the IN718 part of the investigated weld.

Introduction

Inconel 718, or short IN718, was developed in the 1950s for gas turbine applications and is still today the work-horse nickel-iron-chromium alloy for a variety of parts for aero-engine applications such as disks, shafts, blades, vanes, casings and fasteners. IN718 obtains its desired properties through a heat-treatment, which leads primarily to the precipitation of gamma-prime (γ') and gamma-double-prime (γ'') for strengthening, and delta (δ) phase for grain size control [1]. The standard processing, as used for the IN718 material in this work, involves forging, solutionizing in the temperature range 955°C to 985°C and two step aging; 720°C, 8h, cooling to 620°C with 50°C/h and holding at 620°C for another 8h followed by air cooling.
Parts for rotating applications in aero-engines such as disks or BLISKs are normally combined to a bigger component such as a rotor-drum as shown in figure 1. Depending on the temperatures and/or loads within the component this can necessitate joining dissimilar materials. Material combinations realized at MTU Aero Engines for such applications are among others IN718 with IN718, UDIMET® 720LI (U 720LI), and René® 88DT (René88DT). Furthermore, design

limitations can lead to the need of dual material parts, as seen in the tieshaft of one of MTU's latest high pressure compressor designs. Within this part INCOLOY® alloy 909 (Incoloy909) and IN718 are combined to meet the requirements for strength and thermal expansion [2]. Often the only possible joining method is inertia friction welding due to material selection, design and/or space considerations.
Inertia friction welding (inertia welding) is a pressure welding process allowing high strength joints being produced with high reproducibility. The necessary weld-heat is produced by friction and the bonding results from complex plastic deformation below the melting point. Welding of dissimilar materials is possible and the strength of these joints reaches or even exceeds that of the base materials being bonded. In the application area of rotating components for aero-engines, inertia welding is a common practice to join titanium and nickel alloys [3].

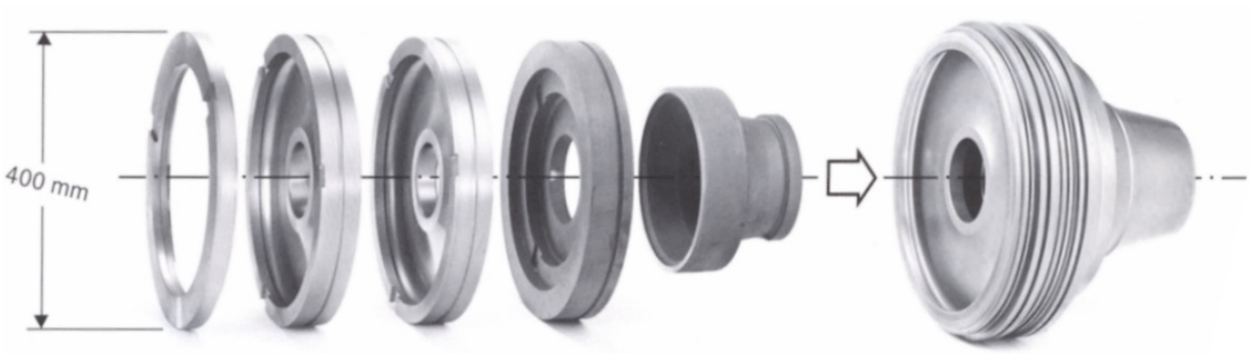

Figure 1. Example of an inertia welded rotor-drum consisting of 5 single parts

The following work summarizes investigations of inertia welding IN718 with alloys Incoloy909, U 720LI, René88DT and itself. The influence of various post-weld heat-treatments on the microstructure and hardness and some relevant mechanical properties as tensile and low cycle fatigue properties are described. The focus in this work is on the IN718 part of the investigated welds.

Experimental

Ring shaped specimens with various dimensions of fully heat-treated IN718, U 720LI, Rene88DT and Incoloy909 were joined by inertia welding; the IN718 material used was coming from two heats fulfilling MTU's specification requirements. The microstructure in the welded zone was investigated by optical microscopy and transmission electron microscopy with the focus on the IN718 side of each weld. Different post-weld heat-treatments (PWHT1-4) were evaluated by microstructural investigations, hardness measurements, tensile tests and load controlled low cycle fatigue tests. The results of the mechanical tests are described in terms of the microstructural changes observed in the welded zones.
A more detailed view of the Incoloy909 side of the Incoloy909-IN718 joint can be found in [4].

Metallurgical Characterization

The changes in the microstructure were characterised using optical (OM) and transmission-electron (TEM) microscopy. All metallurgical characterization has been made on sections cut perpendicular to the joining plane.
Figure 2 shows the microstructure of the IN718 base material. The grain size is about 10µm – 15µm (Fig. 2a, b) and contains δ-phase on the grain boundaries (Fig. 2c). The γ''-phase precipitates are homogeneously distributed throughout the material (Fig. 3a, b).

Figure 4 shows cross sections of the IN718-Incoloy909 (Fig. 4a) and the IN718-René88DT (Fig. 4b) weld, respectively. These two cross sections were selected as Incoloy909 has the lowest and René88 the highest high temperature capability. Visible is the characteristic flash formation for inertia welds caused by the material squeezed out during the upsetting part of the welding process. The differences in size of the flashes within each weld-pair indicate the softer material (= bigger flash), in case of the IN718-Incoloy909 weld it is Incoloy909 and in case of the IN718-Rene88 weld it is the IN718, respectively. The two materials in each weld, the plastically and the heat affected zones (HAZ) are clearly distinguishable by their different etching behavior.

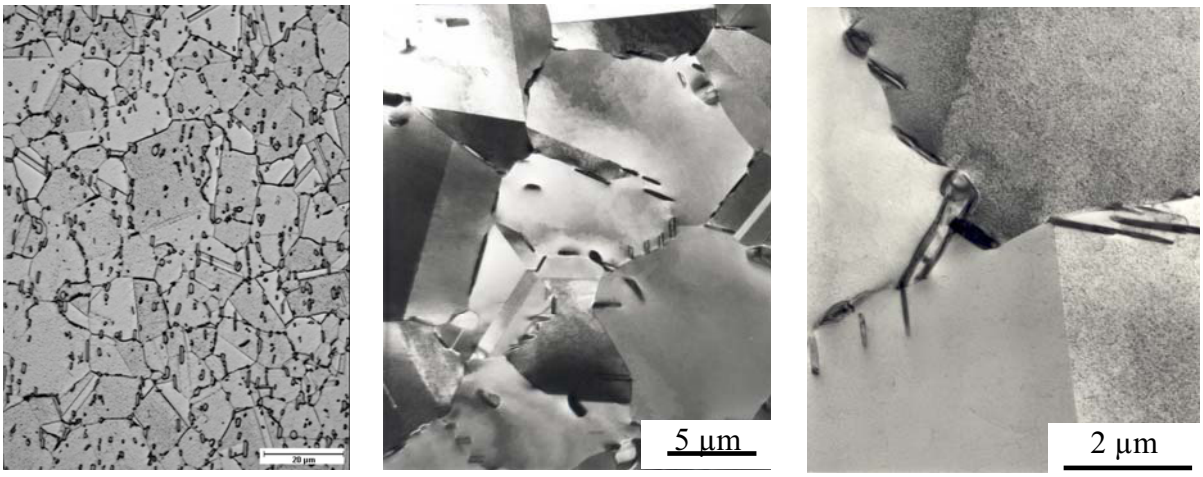

a) OM b) TEM c) TEM

Figure 2. Typical microstructure of the IN718 base material

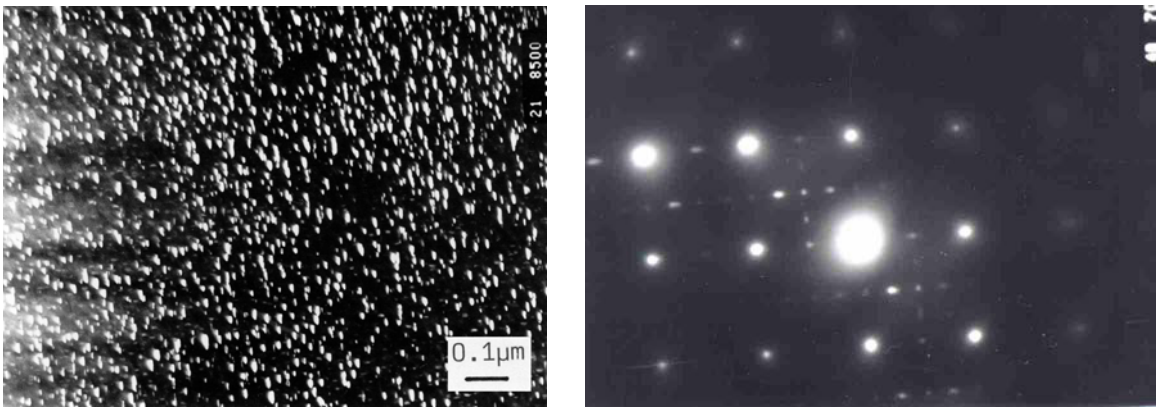

a) b)

Figure 3. TEM micrographs of the IN718 parent material showing
a) γ'' precipitates homogeneously distributed (dark field image).
b) Corresponding (100)-diffraction pattern

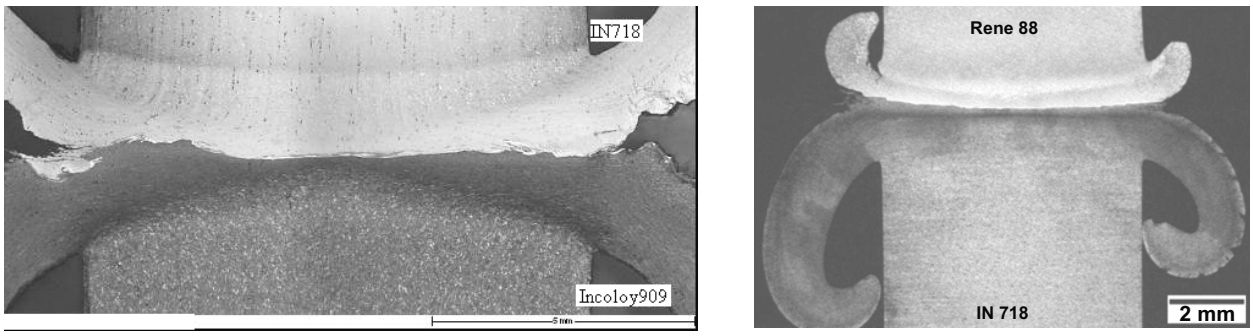

a) IN718 – Incoloy909 b) IN718 – Rene88DT

Figure 4: Cross sections of typical inertia welds; OM

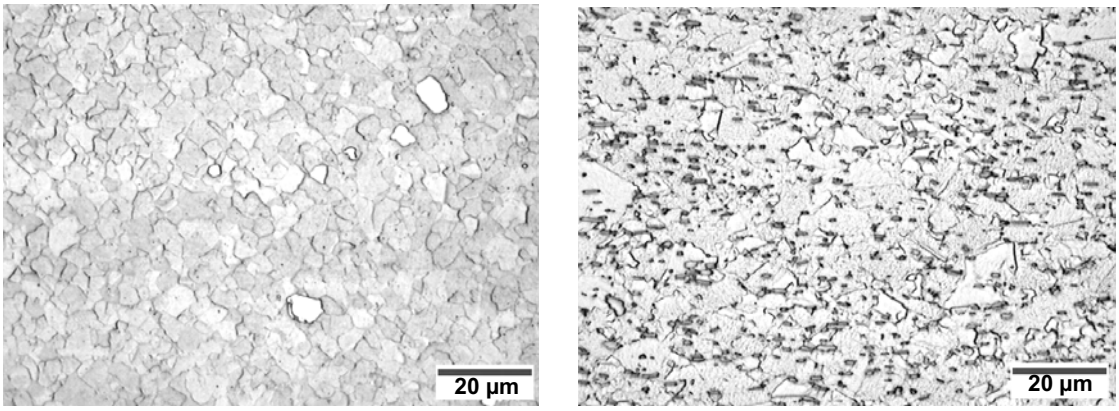

a) weld seam b) heat affected zone

Figure 5. IN718 grain size in the vicinity of the weld

Independent of the weld-combination, the IN718 material shows identical changes in the microstructure. The weld zone of IN 718 has a total thickness of 1 to 1.5 mm in mid-diameter. The weld seam with a thickness of approx. 200µm has a very fine grain size of 3µm to 5µm (Fig. 5a), due to the full recrystallisation of the microstructure during the welding. Within the heat affected zone the grain size increases steadily to about 10 - 15 µm, which corresponds to the grain size of the base material, Figures 5b and 2a. The δ-phase, present in the base material and in the heat affected zone, has been dissolved in the weld seam. Further analysis of the changes in the IN718 material within the weld zone in the as-welded and in different post-weld heat treated conditions were performed using transmission electron microscopy.

The inertia welding process leads to the dissolution of the δ particles in the heat affected zone at distances of up to 350 µm from the weld seam. Figure 6a shows the absence of these δ particles at a distance of 300 µm from the weld seam; whereas at a distance of 500 µm the δ particles are still present (Fig. 6b). The γ'' particles on the other hand are dissolved at distances of up to 500 µm from the weld seam. This is confirmed by the diffraction pattern presented in Figure 7 which shows no superlattice reflections.

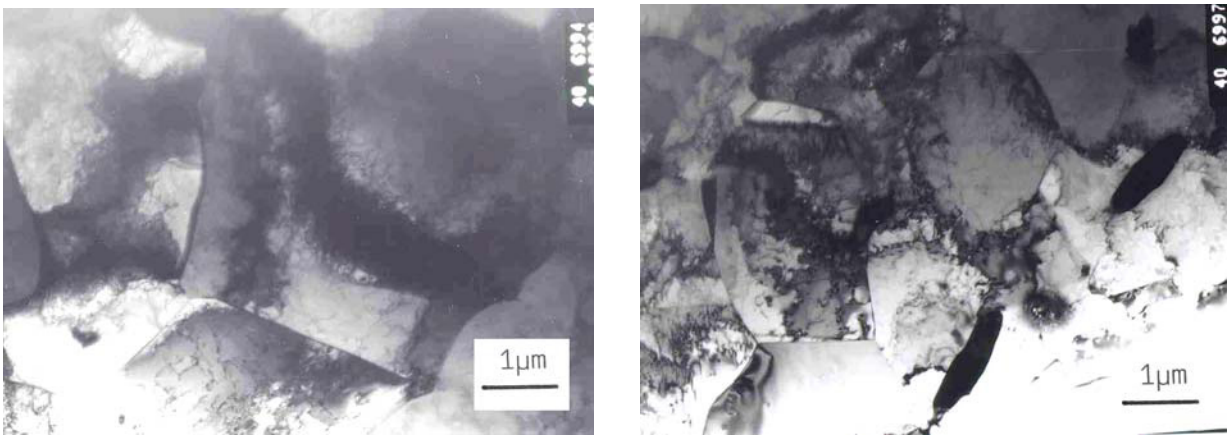

a) b)

Figure 6. TEM micrographs of the IN 718 material in the as-welded condition at

a) a distance of 300 µm from the weld seam where δ precipitates are completely dissolved

b) a distance of 500 µm from the weld seam where δ precipitates are still present

Figure 7. TEM (100)-diffraction pattern of the IN 718 material in the as-welded condition at a distance of 500 µm from the weld seam where γ'' precipitates are completely dissolved (no superlattice reflections)

Furthermore the influence of two post-weld heat-treatments on the microstructure were investigated, PWHT1 and PWHT2 respectively. Neither PWHT1 nor PWHT2 show an influence on the grain size (approx. 3µm) or the distribution of the δ-phase (no δ-phase up to a distance of 350µm from the weld-plane). However, both PWHTs lead to the precipitation of fine γ'' (or γ')-particles in the heat-affected-zone; the size increasing from below 10nm after PWHT1 (Figure 8) to 10-12nm after PWHT2 (Figure 9), nearly comparable to the size as observed in the base material. PWHT3 and 4 are leading most likely to γ'' (or γ')-precipitation patterns within the heat affected zone similar to the base material as they involve heat-treatment times and/or temperatures closer to the full heat treatment cycle (solution treated plus aged = STA) when compared to PWHT1 and 2.

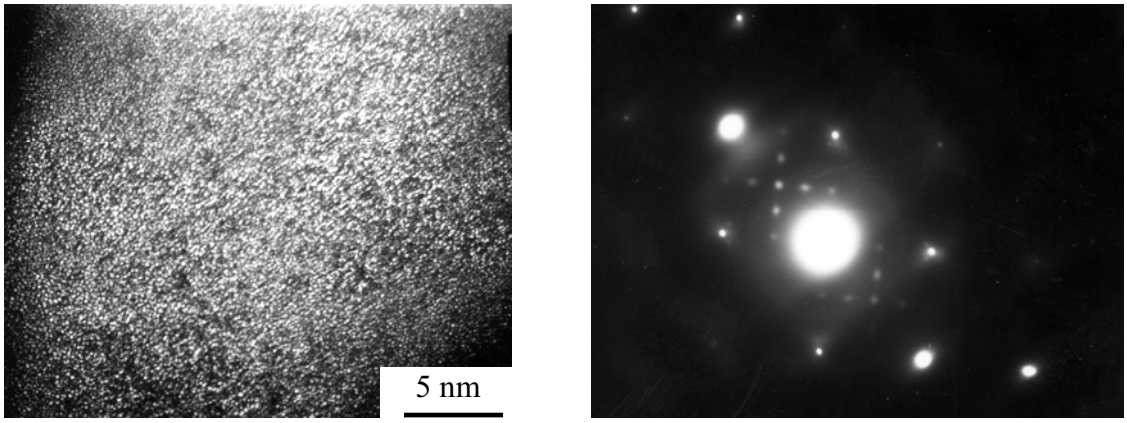

a) b)

Figure 8. TEM micrographs of the IN718 material in the heat-affected-zone after PWHT1:
a) γ'' precipitates homogeneously distributed (dark field image).
b) Corresponding (100)-diffraction pattern

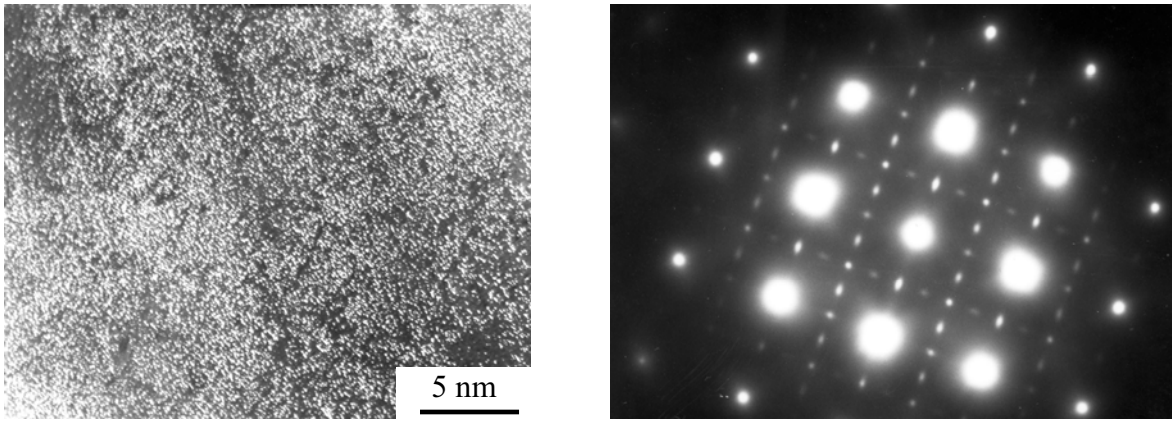

a) b)

Figure 9. TEM micrographs of the IN718 material in the heat-affected-zone after PWHT2
a) γ'' precipitates homogeneously distributed (dark field image).
b) Corresponding (100)-diffraction pattern

Mechanical Characterization

Hardness Measurements

The hardness measurements (HV 0.5) were performed in mid-diameter across the welds for various welded material combinations and post-weld heat-treated conditions. Figure 10 shows the distribution of the hardness for the 4 material combinations in the condition without a PWHT, Figure 11 the distribution of the hardness in the IN718-IN718 weld after PWHT1 and Figure 12 the distribution of the hardness in the Incoloy909-IN718 welds after PWHT3 and PWHT4.
Independent of the specific weld combination the IN718 material shows the same reaction in the hardness values in the weld-plane and the HAZ. The hardness drops from about $450HV_{0.5}$ for the base material down to approx. $300HV_{0.5}$ in the weld-plane (Fig.10) due to the absence of γ'' particles in the as-welded condition. Furthermore the distribution of the hardness between 1mm and 2mm on the IN718 side of the weld indicates a wider HAZ within IN718 for the weld combination with Incoloy909 when compared to that with René88DT, which is also observable in the two metallographic cross sections (Fig.4).
In Figures 11 and 12 the hardness for welded material with an additional full heat treatment cycle (annealing plus 2 step ageing = STA) is shown as the highest possible level. PWHT1 leads to an increase in hardness in the HAZ by $50HV_{0.5}$ and by $100HV_{0.5}$ directly in the weld plane; the increase is mainly a consequence of the precipitated γ''-particles, an additional contribution comes from the very fine grain-size in the weld plane.
PWHT3 and 4 restore the full hardness similar to the STA condition on the IN718 side of the weld as shown in Figure 12 for the IN718-Incoloy909 weld. The increase in hardness towards the weld plane is due to the smaller grain size in this area as compared to the grain size of the base material.

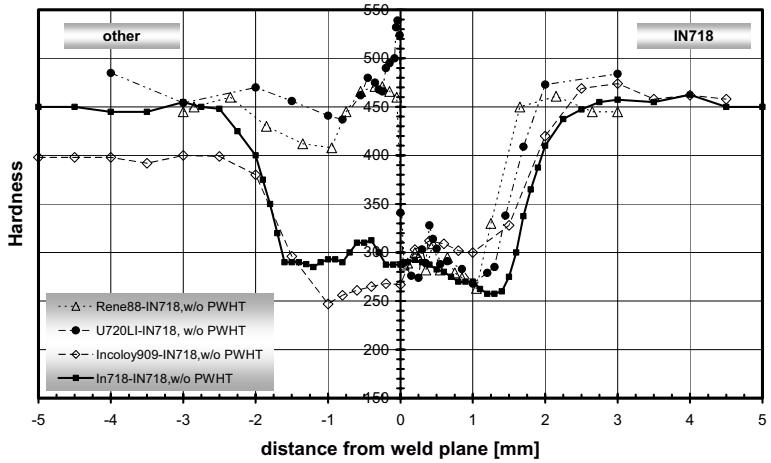

Figure 10. Distribution of the hardness across the welds in the conditions without a post-weld heat-treatment.

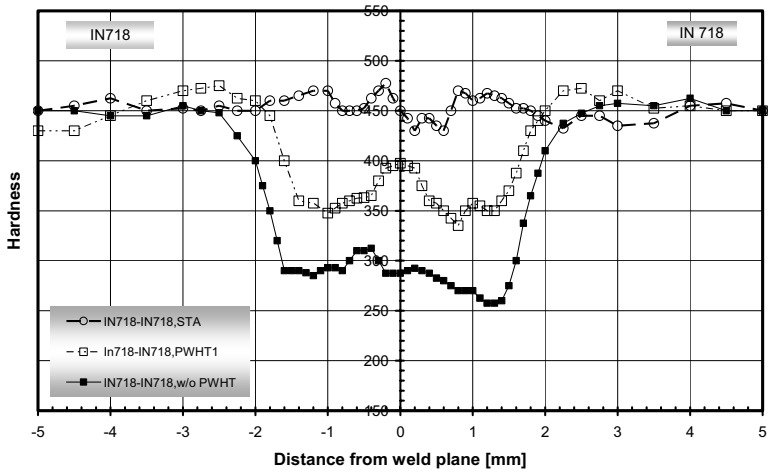

Figure 11. Influence of various post-weld heat-treatments on the hardness in IN718-IN718 welds.

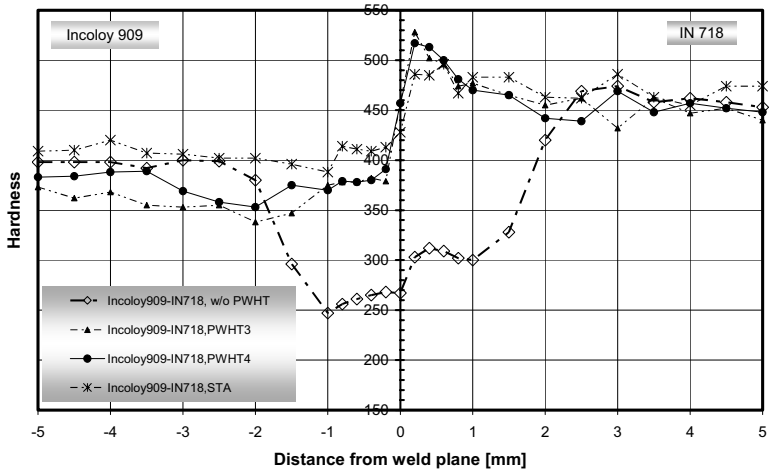

Figure 12. Influence of various post-weld heat-treatments on the hardness of Incoloy909-IN718 welds.

Tensile Properties

Tensile tests were performed for various conditions at 20°C and 650°C and additionally at 450°C for the IN718-Incoloy909 weld-combination. Fig. 13 shows yield strength (YS) and ultimate tensile strength (UTS) of the weld combination IN718-IN718 after PWHT1, PWHT2 and PWHT3 in comparison to typical IN718 data (lines). A similar comparison is made for the mixed welds in Fig. 14.
The results of the welded conditions are plotted at the given test temperature in a window of +/- 10°C to separate the symbols for better clarity.
Apart from the weld combination IN718-Incoloy909 failure occurs on the IN718 side of the weld at strength values typical or close to typical values of IN718. Failure in the IN718-Incoloy909 weld occurs on the Incoloy909 side of the weld in the Incoloy909 base material at typical strength values of Incoloy909 [4] and will therefore not be discussed here.
Those welds which were post-weld heat-treated to PWHT1 (IN718-IN718, Fig. 13, and IN718-U720LI, Fig. 14) failed at strength values below the typical IN718 level and also below those welds with PWHT2 and PWHT3. The lower strength in the HAZ of IN718 after PWHT1 is a consequence of the smaller γ''-particles after PWHT1.

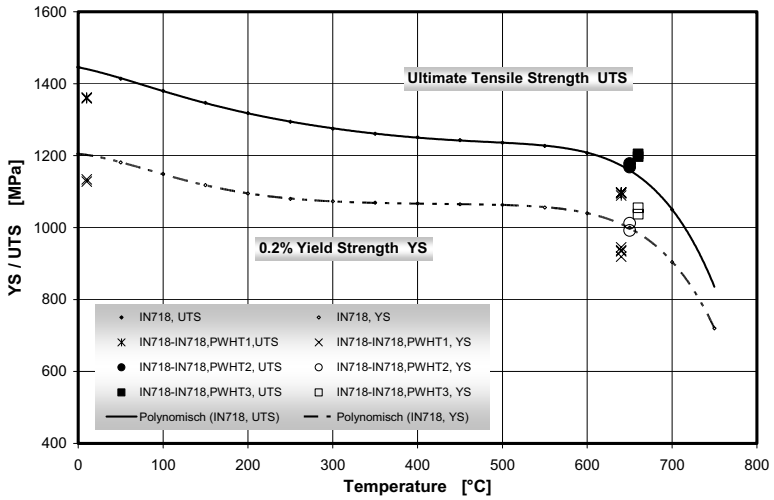

Figure 13. Influence of various PWHTs on YS and UTS of IN718-IN718 welds.

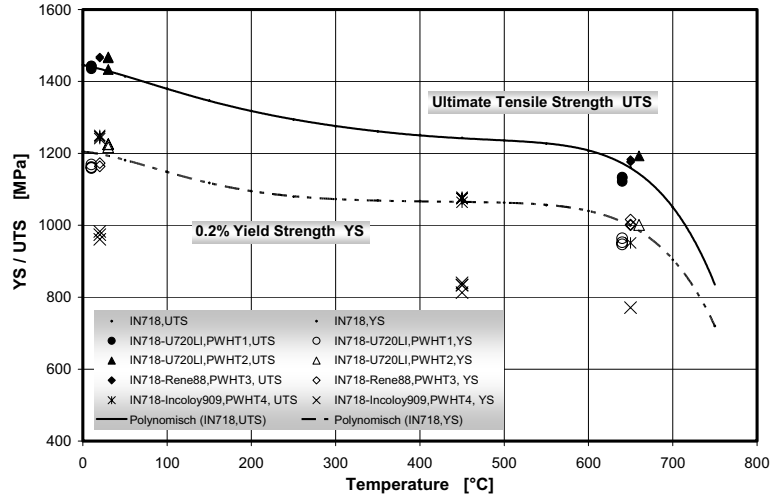

Figure 14. Influence of various PWHTs on YS and UTS of mixed IN718 welds.

Low-Cycle-Fatigue

Low-cycle-fatigue (LCF) tests have been performed as load controlled tests at 600°C in air with an R-Ratio of R = 0 and a frequency of f = 1 Hz using a sinusoidal waveform. The LCF tests for the condition IN718-Incoloy909 were performed at 400°C and can be found in [4].
The LCF-results in Fig. 15 show a similar ranking for the different PWHTs as observed for the hardness or the tensile strength. Welded specimens with PWHT1 fail for a specific cyclic-life at lower maximum stresses than welded specimens post-weld heat-treated to PWHT2 or PWHT3, respectively.
Failure in the all conditions occurred on the IN 718 side of the weld.

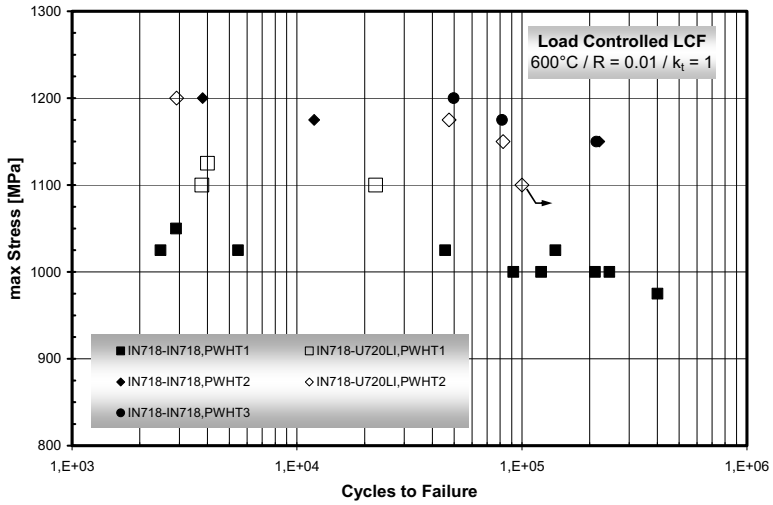

Figure 15. Influence of various post-weld heat-treatments on the LCF-life in various IN718 welds.

Conclusions

Ring shaped specimens with various dimensions of fully heat-treated IN718, U 720LI, Rene88DT and Incoloy909 were joined by inertia welding with IN718. Inertia welding of these combinations is possible and after applying a post-weld heat-treatment the joints reach strength levels close to or equal to the strength level of the weaker of the two base materials. In the case of the Incoloy909-IN718 weld this is the Incoloy909 material, in all other combinations IN718 is the weaker material.
The inertia welding process influences only a small volume of the material adjacent to the weld plane. Within this volume, the plastic deformations and the cooling rates are high and lead in conjunction with a post-weld heat-treatment to the following effects on the IN718 side of the weld:

- The welding process leads to dissolution of the δ-phase for distances up to 350µm from the weld plane and up to 500µm for γ''-particles. Furthermore recrystallisation during the weld process leads to a grain size of approx. 3µm in the weld seam compared to 10µm to 15µm in the IN718 base material. The dissolution of the γ''-precipitates leads to a drop in hardness from approx. 450$HV_{0.5}$ in the IN718 base material to approx. 250 to 300$HV_{0.5}$ in the weld plane.
- Post-weld heat-treatments without a re-solutionizing part in the heat-treatment cycles as the investigated PWHT1 to 4 have no influence on the grain-size or the δ-phase distribution within the HAZ/PAZ. Depending on the time and /or temperature chosen, the

PWHTs influence only the amount and size of the γ''-particles precipitated and thereby directly the strength of the IN718 material adjacent to the weld plane.

Acknowledgments

A part of this work was funded by the Ministry of German Economics and Labor (BMWA). Some of us (OR, DH and SN) appreciate the help of Dr. U. Knott from MTU Aero Engines for welding the specimens and discussion.

Reference

[1] Special Metals Data Sheet „INCONEL® alloy 718“, Publication Number SMC-045, Special Metals Corporation, 2004, 1-28

[2] W. Waschka, K. Rued, W. Humhauser, M. Metscher, A. Michel, „ATFI-HDV: Design of a New 7 Stage Innovative Compressor for 10 – 18 lbf Thrust”, ISABE-2005-1266

[3] P. Adam, Fertigungsverfahren von Flugtriebwerken, 1st ed., Birkhaueuser Verlag, Basel, Switzerland, 1998, p.165

[4] O. Roder, J. Albrecht, G. Luetjering, “Microstructure and Mechanical Properties of An Inertia Welded INCOLOY Alloy 909 – INCONEL Alloy 718 Joint for Rotating Applications”, submitted to WELDS 2005, Int. Conference on Design, Testing, Assessment and Safety of High Temperature Welded Structures, September 8-9, 2005, Geesthacht (Hamburg) Germany, to be published